Available online at www.sciencedirect.com

SciVerse ScienceDirect

Energy Procedia 18 (2012) 1611 – 1623

Energy Procedia

Environmental effects on the performance of nanocrystalline silicon solar cells

A. Guechi[a], M. Chegaar[b] and M. Aillerie[c]

[a]*Institute of Optics and Precision Mechanics, Ferhat Abbas University, 19000, Setif, Algeria*
[b]*Department of Physics, Faculty of Sciences, Ferhat Abbas University, 19000, Setif, Algeria*
Email : ab_guechi@yahoo.fr, chegaar@yahoo.fr
[c]*Laboratoire Matériaux Optiques, Photonique et Systèmes (LMOPS) - EA 4423, Université Paul Verlaine-Metz et Supélec, 2 Rue E.Belin, F-57070 Metz Cedex, France*
E.mail: aillerie@metz.supelec.fr

Abstract

In this paper the global, direct and diffuse solar radiation incident on solar cells is simulated using the spectral model SMARTS2, for varying environmental conditions on the site of Setif. The effect of changes in total intensity and spectral distribution on the short circuit current and efficiency of nanocrystalline silicon (*nc*-Si: H) is examined. The results show a reduction in the short circuit current due to increasing turbidity. It is 27.06% and 67.97% under global and direct radiation respectively. However it increases under diffuse radiation. This increase is about 53.97%. Increasing albedo leads to an increase in the short circuit current of 5.70% and 27.05% for global and diffuse solar radiation, respectively and it is not influenced under direct solar radiation. The performance of the cells is notably reduced, both in terms of efficiency and open circuit voltage, with increasing air mass. It is about 81.86%, 37.47% and 94.18% for global, diffuse and direct solar radiation respectively.

Keywords: Thin film, (*nc*-Si:H) solar cells, efficiency, environmental parameters.

1. Introduction

The traditional development of photovoltaics has been based on crystalline-silicon wafer technology. A new approach arises based on the possibility to grow silicon in the form of a thin film on a given substrate. Thin film technology introduces completely novel concepts and challenges in silicon photovoltaics. Low temperature processes particularly adequate for large-area devices open up not only important cost reduction potential, but also new possibilities such as making semi transparent or flexible modules. Additional important features are highly automated production system, an enormous potential for building integration, a good performance at realistic working temperatures and an excellent durability

 doi:10.1016/j.egypro.2012.05.096

in outdoor conditions among others [1]. The option for thin film crystalline silicon has been discarded for photovoltaic applications due to the relatively poor optical absorption of crystalline silicon. Compared with other thin-film solar cell technologies, thin-film silicon has the advantage of constituting an industrially mature technology and of being based on raw materials which are present in abundance in the earth's crust. Furthermore, small grain silicon films can be grown at moderate temperatures allowing the use of low cost foreign substrates such as glass or even transparent polymer foils [2].

Nomenclature

STC	standard testing conditions
SMARTS	Simple Model of Atmospheric Radiative Transfer of Sunshine
η	conversion efficiency
P_i	incident irradiation (W/m^2)
$E(\lambda)$	beam irradiance, diffuse and global irradiance in the 300-1100 (W/m^{2}nm)
S	area (cm^2)
I_{sc}	short circuit current (mA)
V_{oc}	open circuit voltage (V)
FF	fill factor
n	ideality factor
I_s	saturation current (A)
J_{sc}	short circuit density (mA/cm^2)
$SR(\lambda)$	spectral response
AM	air mass
Turb	turbidity
Albd	albedo
WV	water vapor (cm)

Therefore, microcrystalline and nanocrystalline silicon arise as very promising candidates for the foreseeable future. Several techniques are used for such deposition, for example plasma-enhanced chemical vapour deposition (PECVD) is clearly outstanding given its widespread use and success. Recently, very-high-frequency (VHP PECVD) and hot-wire CVD have appeared as very promising and fast developing alternatives with important potential and actual advantages [3].

Manufacturers report photovoltaic module power output at standard testing conditions (STC), which correspond to 1000 W/m^2, 25°C, air mass 1.5 and normal incidence. In real operating conditions, the module output is strongly affected by various environmental conditions such as irradiance, temperature and spectral effects [5]. Furthermore the impact of each environmental factor on the energy production varies according to the module technology in use.

The aim of this study is to evaluate the effect of changes in spectral distribution of global, direct and diffuse solar irradiation due to the variation of environmental parameters such as air mass, turbidity, ground albedo on the performance of nanocrystalline solar cells. The components of the solar irradiation striking a nanocrystalline solar cell are estimated using the spectral irradiance model for clear skies SMARTS2. The variation of the common performance namely short circuit current, fill factor, open circuit voltage, and efficiency are shown and discussed.

2. Modeling Procedure

2.1. The SMARTS model

Accurate predictions of incident solar radiation are necessary in many different disciplines, not just solar energy applications. Even though it is relatively easy to evaluate irradiances with appropriate broadband radiation models, spectral models provide considerably more flexibility, and normally better accuracy because of the physical nature of their modeling. In many spectrum-dependent applications, they even are the only resource. A number of spectral radiative models have been described or used in the literature and some of these models are reviewed elsewhere [4-6].

The SMARTS2 (Simple Model of Atmospheric Radiative Transfer of Sunshine) model was developed by Gueymard [6-10]. It is based on an extensive revision of the algorithms used to calculate direct, diffuse and global irradiation [11] and consists of a separate parameterization of the different extinction processes involved in the atmosphere. In this model, more accurate transmittance functions for all atmospheric extinction processes are introduced as well as temperature and humidity effects. SMARTS2 is used to generate the solar spectra for the site of Setif (36.18°N, 5.41°E and 1081m) which is characterised by a clear sky most of the time.

2.2. Cell parameters calculation

The fill factor and the conversion efficiency η of the solar cell are associated through:

$$\eta = FF \frac{V_{oc} I_{sc}}{P_i S} \tag{1}$$

Where P_i is the incident irradiation in W/m^2 and is given by:

$$P_i = \int_0^\infty E(\lambda)\, d\lambda \tag{2}$$

With $E(\lambda)$ is the spectral irradiance, S is the area of the device, I_{sc} is the short circuit current and V_{oc} is the open circuit voltage.

The fill factor FF is defined as [12]:

$$FF = \frac{v_{oc} - \ln(v_{oc} + 0.72)}{v_{oc} + 1} \tag{3}$$

Where:

$$v_{oc} = \frac{V_{oc}}{n\left(\frac{kT}{q}\right)} \tag{4}$$

The open circuit voltage is given by:

$$V_{oc} = n\frac{kT}{q}\ln\left(\frac{I_{ph}}{I_s}+1\right) \tag{5}$$

The ideality factor, n, and the saturation current, I_s, are computed from the I-V characteristics using an approach that involves the use of an auxiliary function and a computer-fitting routine [13].

The short circuit density J_{sc} of device, which is the value of the photocurrent density, is directly linked to the spectral irradiance *E (λ)* and can be calculated as:

$$J_{sc} = \int E(\lambda)\ SR(\lambda)\ d\lambda \tag{6}$$

Where *E (λ)* is the energy of the incident light and *SR (λ)* is the measured spectral response at the given wavelength, *λ*. Figure 1 shows the measured spectral response of the hydrogenated nanocrystalline silicon (nc-Si: H) [14] solar cell considered in this work. It is clear that nanocrystalline silicon (nc-Si) cells respond in the range 300-1100nm.

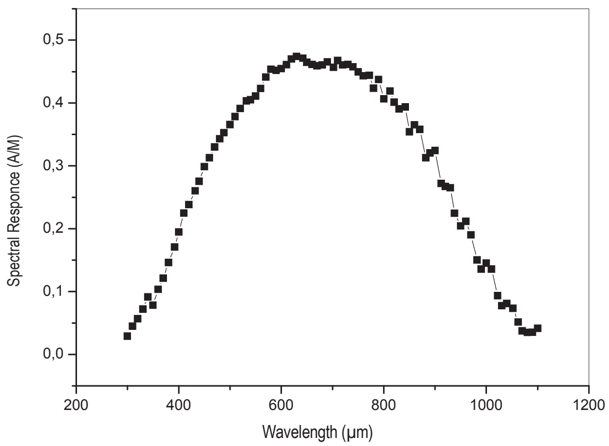

Fig. 1. Spectral response of (nc-Si: H) solar cell

3. Resultats and discussion

3.1. Effect of turbidity

Turbidity is the optical property that causes light to be scattered and absorbed rather than transmitted in straight lines through the atmosphere. Atmospheric turbidity is associated with atmospheric aerosol load. These particles are either of natural sources (such as volcanic eruptions, dust storms, forest and grassland fires, sea spray, etc.). For an ideally dust free atmosphere the turbidity is zero, and a perfect opaque sky has a turbidity of 1. Typical value of turbidity can vary between 0 to about 0.4. An increase in the concentration of aerosols in some urban regions caused by human activity has a significant impact on the environmental quality of the cities, which makes the air turbid with lower visibility. In addition, aerosols play an important role in absorption and scattering of solar radiation, as well as in the physics of clouds and precipitation. Therefore, atmospheric turbidity is not only an important factor for monitoring the air pollution, but also in meteorology, climatology and for designing of solar energy systems.

Fig. 2 shows the influence of turbidity on the different considered solar irradiance. The output current is reduced but in different proportion for each component of solar irradiation. The reduction in the short circuit current due to increasing turbidity is 27.06% and 67.97%, respectively for global and direct solar irradiance when the turbidity increases from 0.1 to 0.40. However, the increase percentage in current is 41, 91% for diffuse solar irradiance. A general summary of the results is presented in Table 1.

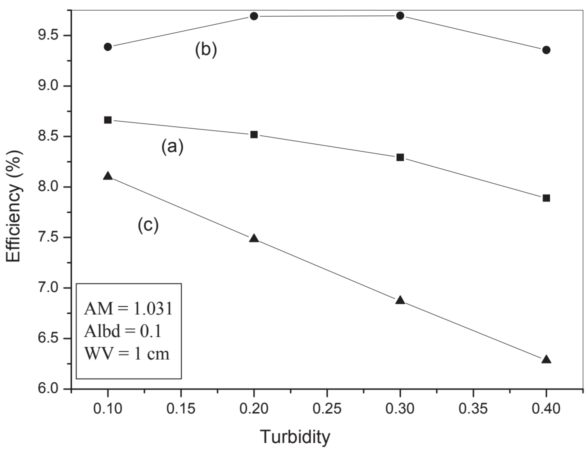

Fig.2. Efficiency as function of turbidity under global (a), diffuse (b) and direct (c) irradiation

Table 1. Influence of the turbidity on the performance of (nc-Si: H) under global, direct and diffuse solar irradiation

Irradiance	Turbidity	J_{sc} (mA /cm^2)	V_{oc} (V)	FF
Globale	0.1	27.7147	0.4766	0.7512
	0.2	26.2317	0.4747	0.7506
	0.3	24.0865	0.4717	0.7495
	0.4	21.0123	0.4670	0.7478
Direct	0.1	22.5057	0.4695	0.7487
	0.2	17.8239	0.4613	0.7457
	0.3	14.1671	0.4534	0.7428
	0.4	11.3210	0.4456	0.7398
Diffuse	0.1	5.2590	0.4187	0.7288
	0.2	8.4077	0.4353	0 .7357
	0.3	9.9104	0.4410	0.7380
	0.4	9.6913	0.4402	0.7377

3.2. Air mass effect

The amount of atmosphere (air thickness) traversed by a sunray as it travels from the top of the atmosphere to a point on the Earth's surface is often called the air mass. The air mass is the ratio of the mass of the atmosphere through which beam radiation passes to the mass it would pass through if the sun was at the zenith. It may be expressed as a multiple of the path traversed to a point at sea level with the sun at zenith. The longer the path through the atmosphere, the greater the air mass encountered by the sunray and the greater the attenuation. Since there are no gases or aerosols in space between the Sun and the top of the Earth's atmosphere , the air mass at the top of the atmosphere is zero (AM0). When the sun angle is 90°, the air mass from the top of the atmosphere is defined as having a value of one (AM1). Air mass 1.5 corresponds to a solar elevation of about 42°.

The air mass along any path from the top of the atmosphere to the Earth's surface is approximately related to the sun angle. When the angle of the sun from zenith (directly overhead) increases, the air mass increases approximately by the secant of the zenith angle.

The variation of the short current, open circuit voltage, fill factor and efficiency as function of the air mass are illustrated in Table 2. The short circuit current decreases with increasing air mass, this reduction is about 81.86%, 37.47% and 94.18% respectively for global, diffuse and direct solar radiation when the air mass increases from AM= 1.031 to AM = 4.431. The efficiency decreases with increasing air mass. This is illustrated in Fig. 3.

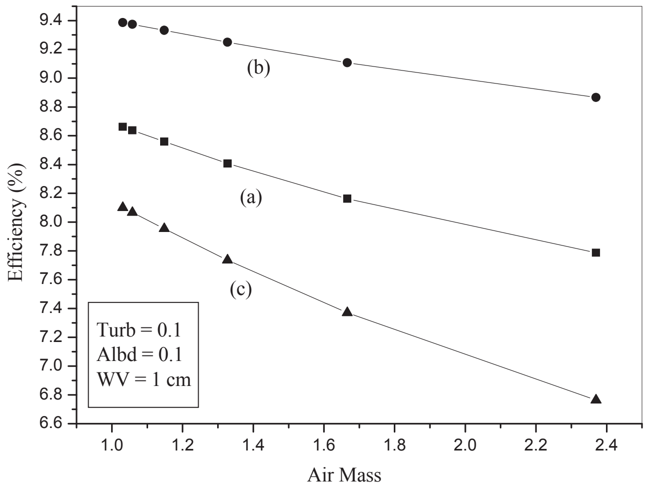

Fig.3. Efficiency as function of air mass under global (a), diffuse (b) and direct (c) irradiation

Table 2. Influence of air mass on the performance of (nc-Si: H) under global, direct and diffuse solar irradiaion

Irradiance	Air Mass	J_{sc}(mA /cm^2)	V_{oc} (V)	FF
Global	1.031	27.7147	0.4766	0.7512
	1.058	26.9327	0.4756	0.7509
	1.148	24.6159	0.4725	0.7497
	1.327	20.0123	0.4669	0.7478
	1.666	16.0650	0.4577	0.7444
Direct	1.031	22.5057	0.4694	0.7487
	1.058	21.7770	0.4683	0.7483
	1.148	19.6275	0.4647	0.7469
	1.327	16.2280	0.4581	0.7445
	1.666	11.8583	0.4472	0.7404
Diffuse	1.031	5.2090	0.4187	0.7288
	1.058	5.1557	0.4184	0 .7287
	1.148	4.9884	0.4172	0.7282
	1.327	4.6866	0.4151	0.7273
	1.666	4.2067	0.4113	0.7256

3.3. Albedo effect

Albedo is the diffuse reflectivity or reflecting power of a surface. It is defined as the ratio of reflected radiation from the surface to incident radiation upon it. Being a dimensionless fraction, it may also be expressed as a percentage, and is measured on a scale from zero for no reflecting power of a perfectly black surface, to 1 for perfect reflection of a white surface. Albedo depends on the frequency of the radiation. In general, the albedo depends on the directional distribution of incoming radiation. Ice, especially with snow on, has a high albedo. Most sunlight hitting the surface bounces back towards space. Water is much more absorbent and less reflective.

The variations of the efficiency as a function of albedo at Setif are presented in Fig 4. Table 3 shows the influence of the albedo on the (nc-Si: H) solar cells parameters i.e. the short current, open circuit voltage and fill factor at Setif. As can be seen the efficiency increases with increasing albedo. The short circuit current increase with increasing albedo, this increases are 47.46% when the albedo increases from 0.2 to 0.8.

Table 3. Influence of albedo on the performance of (nc-Si: H) under global, direct and diffuse solar irradiation

Irradiance	Albedo	J_{sc}(mA /cm^2)	V_{oc}(V)	FF
Global	0.1	27.7147	0.4766	0.7512
	0.2	28.0246	0.4770	0.7514
	0.3	28.3419	0.4774	0.7515
	0.4	28.6667	0.4778	0.7516
	0.5	28.9995	0.4782	0.7518
	0.6	29.3405	0.4786	0.7519
Direct	0.1	22.5057	0.4694	0.7487
	0.2	22.5057	0.4694	0.7487
	0.3	22.5057	0.4694	0.7487
	0.4	22.5057	0.4694	0.7487
	0.5	22.5057	0.4694	0.7487
	0.6	22.5057	0.4694	0.7487
Diffuse	0.1	5.2090	0.4187	0.7288
	0.2	5.5188	0.4207	0.7297
	0.3	5.8361	0.4227	0.7305
	0.4	6.1610	0.4245	0.7313
	0.5	6.4938	0.4264	0.7320
	0.6	6.8348	0.4281	0.7328

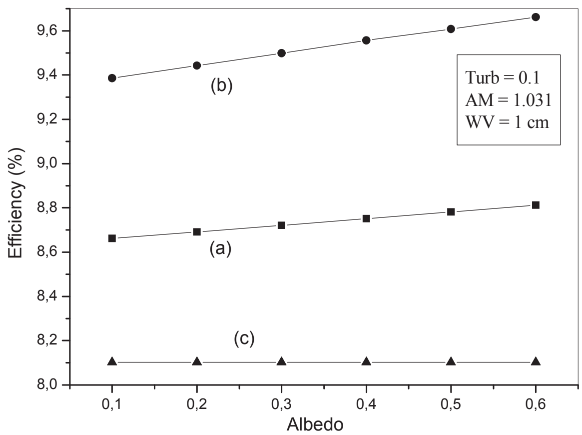

Fig.4. Efficiency as function of albedo under global (a), diffuse (b) and direct (c) irradiation

4. Conclusion

The study of the solar spectral irradiance components and their spectral modification under different environmental conditions has proved to be a significant field of research specifically as regards the air quality in rural areas. This study focused on the solar radiation components and their modification with different environmental factors, and their effects on the performance of (nc-Si: H) solar cells. The global, direct and diffuse solar irradiance are simulated using the spectral irradiance model SMARTS2 for clear skies on the site of Setif (Algeria). The results show that the short circuit current increases with increasing turbidity for diffuse solar irradiance and it decreases for global and direct irradiance. The efficiency decreases with increasing turbidity for global and direct irradiance but for diffuse irradiance the efficiency increases with increasing turbidity. The short circuit current decreases with increasing air mass under global, direct and diffuse solar irradiance. The efficiency increases with increasing albedo for global and diffuse solar irradiance and remains constant for the direct solar irradiance. Besides these purely physical limitations, there are, however, ecological, technological and economical constraints for large scale energy applications. These certainly merit full attention in view of photovoltaic technology assessment.

References

[1] Cárabe J, Gandia J J, thin film solar cell, *Opto Electronics Review* **12**(1), 1-6, 2004.

[2] Pernet P et al, 2nd World Conference on Photovoltaic Solar Energy Conversion, Vienna, 976-979, 1998.

[3] Rath J K, Stannowski B, Van Veenendaal P A T T, Van Veen M K and Schropp R E I. Application of hot-wire chemical vapor- deposited Si:H films in thin film transistors and solar cells. *Thin Solid Films* **395**, 320, 2001.

[4] Gueymard C, Spectral Models, in Solar Energy -The State of the Art, Gordon J, editor , *James & James Pub*., *London*, p. 527-531, 2001.

[5] Gueymard C, Kambezidis H D, Solar spectral radiation. *In: Muneer T, editor*. Solar radiation and daylight models, *2nd Ed, Elsevier* 221-301, 2004.

[6] Gueymard C. REST2: High-performance solar radiation model for cloudless-sky irradiance, illuminance, and photosynthetically active radiation –Validation with a benchmark dataset. *Solar Energy* 82, 272–285, 2008.

[7] Gueymard C, George R. Gridded aerosol optical depth climatological datasets over continents for solar radiation modeling. *Proceedings of the Solar World Congress. International Solar Energy Society, Orlando, FL*, 2005

[8] Gueymard C. SMARTS2, Simple Model of the atmospheric Radiative Transfer of Sunshine: Algorithms and performance assessment. *Report. FSEC-PF-270-95, Florida-Solar Energy Center, Cocoa, FL*, 1995.

[9] Gueymard C. The sun's total and spectral irradiance for solar energy applications and solar radiation models. *Solar Energy*, 76: 423-452, 2004.

[10] Gueymard C. Prediction and Validation of Cloudless Short wave Irradiance Spectra for Horizontal, Titled or Tracking Receivers, *Solar Conference, ASES, Denver Co.,* 2006.

[11] Gueymard C, Myers D R. Evaluation of conventional and high-performance routine solar radiation measurements for improved solar resource, climatological trends, and radiative modeling", *Solar Energy* 83, 171–185, 2009.

[12] Green M A, Solar Cells, Operating Principals, Technology, and System Applications, *Prentice-Hall Inc., Englewood Cliffs*, 1982.

[13] Chegaar M, Azzouzi G, and Mialhe P. Simple parameter extraction method for illuminated solar cells. *Solid-State Electronics* 50, 1234 -1237, 2006.

[14] Guha S, Yang J. High-Efficiency Amorphous Silicon and Nanocrystalline Silicon-Based Solar Cells and Modules. *NREL Final Technical Progress Report,* 520-35092, 2008.

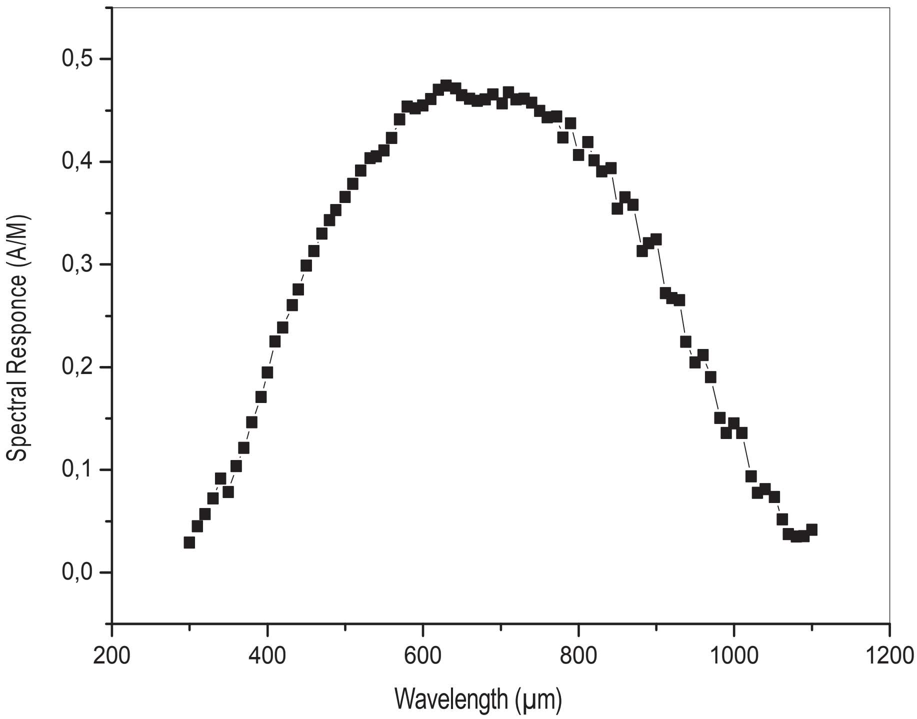

Fig. 1. Spectral response of (nc-Si: H) solar cell

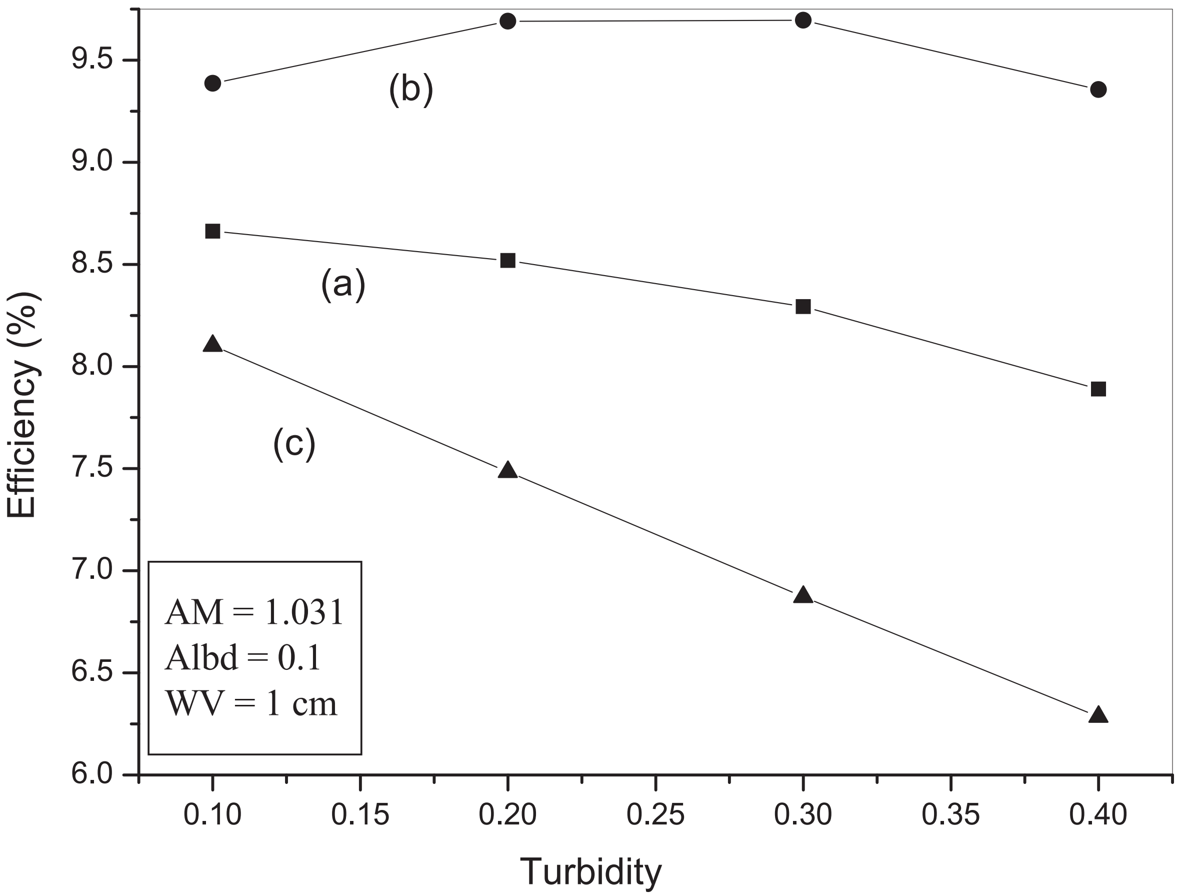

Fig.2. Efficiency as function of turbidity under global (a), diffuse (b) and direct (c) irradiation

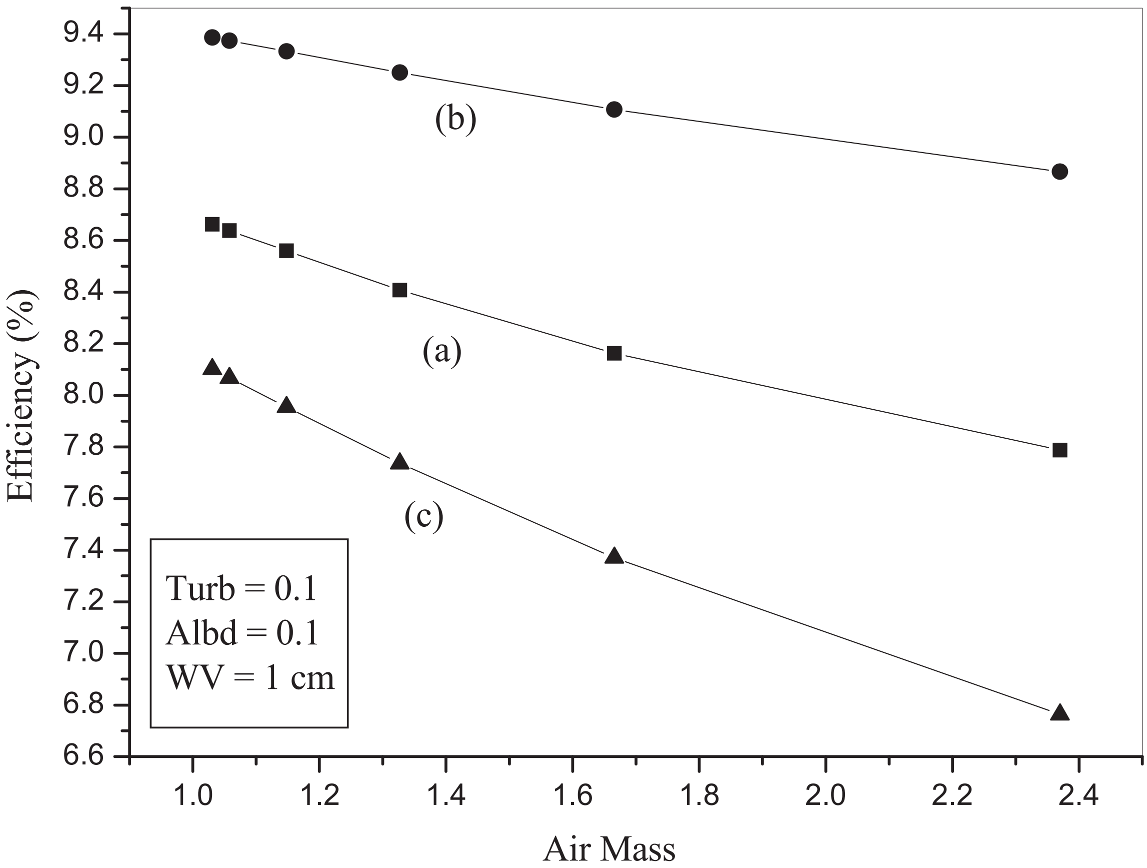

Fig.3. Efficiency as function of air mass under global (a), diffuse (b) and direct (c) irradiation

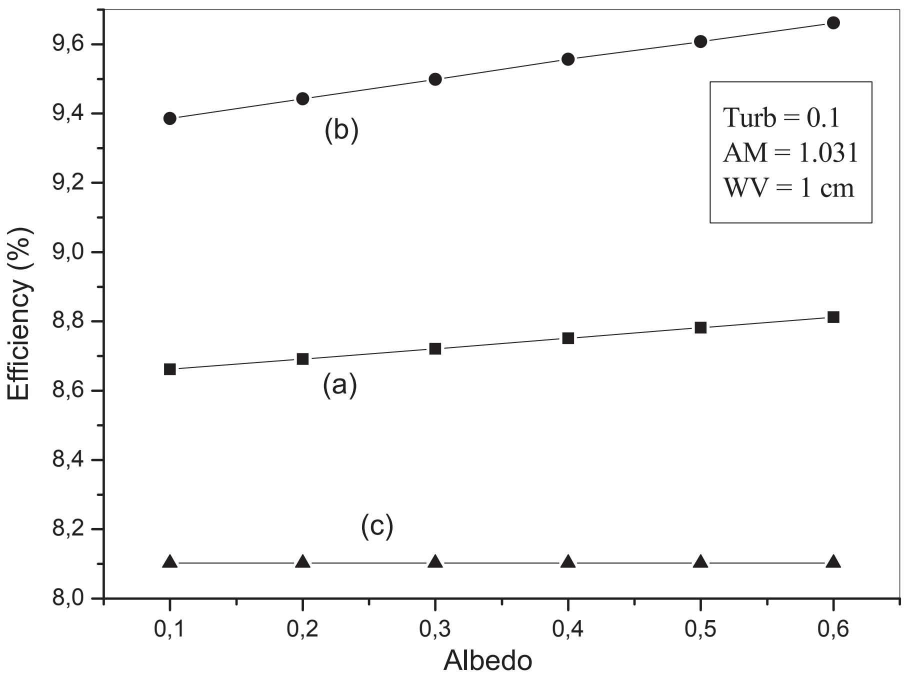

Fig.4. Efficiency as function of albedo under global (a), diffuse (b) and direct (c) irradiation